Loss-of-function mutation in *Mirta22/Emc10* rescues specific schizophrenia-related phenotypes in a mouse model of the 22q11.2 deletion

Anastasia Diamantopoulou[a,b], Ziyi Sun[b], Jun Mukai[b], Bin Xu[a], Karine Fenelon[b,1], Maria Karayiorgou[a,2,3], and Joseph A. Gogos[b,c,2,3]

[a]Department of Psychiatry, College of Physicians and Surgeons, Columbia University, New York, NY 10032; [b]Department of Physiology and Cellular Biophysics, College of Physicians and Surgeons, Columbia University, New York, NY 10032; and [c]Department of Neuroscience, College of Physicians and Surgeons, Columbia University, New York, NY 10032

Edited by Stephen T. Warren, Emory University School of Medicine, Atlanta, GA, and approved May 5, 2017 (received for review September 20, 2016)

Identification of protective loss-of-function (LoF) mutations holds great promise for devising novel therapeutic interventions, although it faces challenges due to the scarcity of protective LoF alleles in the human genome. Exploiting the detailed mechanistic characterization of animal models of validated disease mutations offers an alternative. Here, we provide insights into protective-variant biology based on our characterization of a model of the 22q11.2 deletion, a strong genetic risk factor for schizophrenia (SCZ). Postnatal brain up-regulation of *Mirta22/Emc10*, an inhibitor of neuronal maturation, represents the major transcriptional effect of the 22q11.2-associated microRNA dysregulation. Here, we demonstrate that mice in which the *Df(16)A* deficiency is combined with a LoF *Mirta22* allele show rescue of key SCZ-related deficits, namely prepulse inhibition decrease, working memory impairment, and social memory deficits, as well as synaptic and structural plasticity abnormalities in the prefrontal cortex. Additional analysis of homozygous *Mirta22* knockout mice, in which no alteration is observed in the above-mentioned SCZ-related phenotypes, highlights the deleterious effects of *Mirta22* up-regulation. Our results support a causal link between dysregulation of a miRNA target and SCZ-related deficits and provide key insights into beneficial LoF mutations and potential new treatments.

LoF mutations | 22q11.2 microdeletion | Mirta22/Emc10

Despite substantial progress in the field of psychiatric genetics, the heterogeneity of genetic etiology and the corresponding neural complexity has rendered the task of understanding disease pathophysiology and developing improved treatments rather inauspicious (1). In light of this complexity, there is need to identify convergent neural substrates and underlying molecular mechanisms that can serve as entry points to prevent or reverse disease progression. Along the same lines, identification of genetic mutations or variants that confer protection against disease via loss-of-function effects (LoF), akin to those of a therapeutic agent, hold great promise for devising therapeutic schemes (2-5) to restore or prevent some or all disease symptoms, either in all patients or, more likely, in specific subsets of patients with well-defined genetic lesions of affected pathways. A well-established example is provided by studies of the *PCSK9* locus, where therapeutic agents designed to inhibit PCSK9 were prospectively developed in response to the detected protective effects of *PCSK9* LoF variants on LDL cholesterol levels and coronary artery disease risk (6, 7). Similar success has increasingly been reported in other human diseases (8) (albeit not neuropsychiatric or neurodevelopmental disorders so far) and has prompted efforts to identify additional such advantageous LoF variants (9). However, such studies face a number of challenges due to the scarcity of protective LoF alleles in the human genome, necessitating the use of exceedingly large cohorts of patients and healthy controls or resorting to either founder of consanguineous population, which are more likely to bear an excess of rare, functionally relevant protective variants (5). Another approach to identify such beneficial LoF mutations is to take advantage of animal models that accurately recapitulate validated pathogenic disease mutations. The detailed mechanistic characterization afforded in such model organisms could, in principle, identify genes or genetic pathways triggered by the primary mutation, whose LoF might lead to amelioration of disease severity and progression.

Here, using an extensively characterized animal model of the 22q11.2 deletion, one of the strongest known genetic risk factor for schizophrenia (SCZ) (10, 11), we show that animal models of validated disease mutations can provide important insights into protective-variant biology. Specifically, previous research on the 22q11.2 deletions provided one of the strongest initial indications for a link between miRNA dysregulation and SCZ risk (12, 13). A mouse model carrying a hemizygous 1.3-Mb chromosomal deficiency on chromosome 16 [Df(16)A], which is syntenic to the human 1.5-Mb 22q11.2 microdeletion, demonstrates abnormal processing and levels of brain miRNAs (12). This miRNA dysregulation is due to hemizygosity of *DGCR8*, a component of the "microprocessor" complex that is essential for miRNA production, as well as hemizygosity of miRNA genes residing within the deletion, most notably *mir185* (12, 14, 15).

Significance

Despite substantial progress in the field of schizophrenia (SCZ) genetics, the heterogeneity of genetic etiology and neural complexity has rendered the task of developing improved treatments inauspicious. Thus, there is need to identify convergent neural substrates and underlying molecular mechanisms that can serve the prevention or reversal of disease progression. Our extensive characterization of an animal model of the 22q11.2 deletion, one of the strongest genetic risk factors for SCZ, when combined with a loss-of-function (LoF) mutation for a microRNA-dependent upregulated target, offers a proof of principle for such approaches. Hence, identification of variants that confer protection against disease by disabling protein function via LoF effects holds great promise for devising therapeutic schemes to restore or prevent disease symptoms.

Author contributions: A.D., Z.S., J.M., B.X., K.F., M.K., and J.A.G. designed research; A.D., Z.S., J.M., B.X., and K.F. performed research; A.D., Z.S., J.M., B.X., and K.F. analyzed data; J.A.G. supervised the work; and A.D. and J.A.G. wrote the paper.

The authors declare no conflict of interest.

This article is a PNAS Direct Submission.

[1]Present address: Department of Biological Sciences, University of Texas at El Paso, El Paso, TX 79968.

[2]To whom correspondence may be addressed. Email: mk2758@cumc.columbia.edu or jag90@columbia.edu.

[3]M.K. and J.A.G. share senior authorship.

This article contains supporting information online at www.pnas.org/lookup/suppl/doi:10.1073/pnas.1615719114/-/DCSupplemental.

Colocalization of *DGCR8* and *mir185* within the 22q11.2 locus results in a drastic reduction of the mir185 levels, greater than expected by the 50% decrease in genomic dosage, and results in a derepression of a previously unknown inhibitor of neuronal maturation, *Mirta22* (*Emc10*), whose expression is partly under the control of *mir185*. *Mirta22* is a prenatally biased gene with high expression in embryonic life that subsides after birth. Importantly, the end effect of 22q11.2-related derepression of *Mirta22* expression is evident only in postnatal life in the form of a robust and reproducible increase in Mirta22 postnatal levels compared with wild-type (WT) mice (14). Indeed, postnatal *Mirta22* up-regulation is the major downstream transcriptional effect of the 22q11.2-associated miRNA dysregulation (14), and, given that Mirta22 functions as an inhibitor of neuronal maturation, it may represent a key link in our understanding and manipulating of the chain of events leading from disease risk mutation to behavioral disturbance.

Df(16)A$^{+/-}$ mice show a distinct behavioral and cognitive profile, which includes central constructs affected in SCZ. Specifically, the mice exhibit hyperactivity, decrease in prepulse inhibition (PPI) that is indicative of sensorimotor gating deficits, working memory (WM) abnormalities, social memory (SM) deficits, and associative (fear) memory deficits (12). In addition to the observed behavioral abnormalities, *Df(16)A*$^{+/-}$ mice also show alterations in the dendritic development of cortical neurons, as well as deficits in several forms of prefrontal cortical synaptic plasticity, which also emerge in part due to miRNA dysregulation (16). If the sustained postnatal elevation of *Mirta22* levels hinders normal development of circuits and behaviors, one prediction would be that LoF mutations of *Mirta22* will have beneficial effects, preventing the emergence of at least some of these deficits.

In the present study, we show that genetic reduction of Mirta22 levels rescues key SCZ-related cognitive and behavioral dysfunctions present in the *Df(16)A*$^{+/-}$ mice, as well as several of the underlying synaptic and cellular deficits. Our results suggest that several key behavioral and physiological alterations observed in *Df(16)A*$^{+/-}$ mice can be attributed to the abnormally sustained inhibitory influence of elevated *Mirta22* levels and highlight "protective" elements in the genetic and neural architecture of neuropsychiatric disorders.

Results

Restoration of Mirta22 Levels in the Df(16)A$^{+/-}$ Mice. We hypothesized that abnormally sustained high levels of Mirta22 in the postnatal brain are significant contributors to the phenotypic deficits observed in *Df(16)A*$^{+/-}$ mice. To test our hypothesis, we generated compound heterozygote mice in which the *Df(16)A* deficiency was combined with a LoF *Mirta22* allele, resulting in the reduction of Mirta22 levels and near-normal restoration of its postnatal expression in several brain regions (*SI Appendix*, Fig. S1). We used these mice to test whether reduction of Mirta22 levels and the accompanying relief from its inhibitory influences mitigate cognitive and behavioral dysfunctions present in the *Df(16)A*$^{+/-}$ mice and prevent several of the underlying synaptic and cellular deficits.

Restoration of Mirta22 Levels Prevents Deficits in PPI, WM-Dependent Learning, and SM. Sensorimotor gating deficits in the form of PPI are frequently observed in patients with SCZ. PPI expression is regulated by a wide corticolimbic and brainstem network, upon which prefrontal cortex (PFC) exerts an important neuromodulatory role (17–21). Although sensorimotor gating is not a cognitive process per se, it correlates well with several cognitive domains, such as executive function (22), WM (23–25), and social cognition (26) and likely shares neural substrates with these domains. We have previously shown that *Df(16)A*$^{+/-}$ mice exhibit a robust PPI deficit (12). Analysis by genotype [repeated measures (RM) ANOVA, prepulse × genotype interaction $F(12, 224) = 1.981$, $P = 0.027$; main effect of genotype $F(3, 56) = 8.308$, $P < 0.001$] confirmed our previous result [*Df(16)A*$^{+/-}$ vs. WT, Bonferroni post hoc analysis, $P < 0.0001$; Fig. 1*A*], and revealed an overall prevention of PPI deficit in *Df(16)A*$^{+/-}$*;Mirta22*$^{+/-}$ mice, which is statistically indistinguishable from WT mice [*Df(16)A*$^{+/-}$*;Mirta22*$^{+/-}$ vs. WT, not significant (ns)]. Consistently, *Df(16)A*$^{+/-}$*;Mirta22*$^{+/-}$ mice show significantly increased PPI levels compared with *Df(16)A*$^{+/-}$ mice (Bonferroni post hoc analysis, $P = 0.026$) (Fig. 1*A*). PPI of *Mirta22*$^{+/-}$ mice was indistinguishable from WT littermates. Startle responses and hearing as evaluated by an acoustic startle test did not differ among genotypes (*SI Appendix*, Fig. S2). Thus, the PPI deficit observed in *Df(16)A*$^{+/-}$ mice can be attributed at least partially to the inhibitory influence of elevated Mirta22 levels.

WM is a primary cognitive domain frequently compromised in patients with SCZ, and its restoration is particularly resistant to antipsychotic medication. WM depends on the intact structure and short- and long-range communication, as well as local synaptic plasticity at the PFC (27–29). A deficit in a T-maze version of the delayed nonmatch to sample task for WM is one of the most reproducible and reliable outcome measures in *Df(16)A*$^{+/-}$ mice, which exhibit a delay in acquiring the task (12, 30). We used this task as our first test of the effects of Mirta22 reduction on cognitive performance. Our results corroborated the known spatial WM-dependent learning deficit of *Df(16)A*$^{+/-}$ mice [post hoc Bonferroni comparisons; *Df(16)A*$^{+/-}$ vs. WT, days to criterion: $P < 0.001$; Fig. 1*B*] and revealed a prevention of this specific WM deficit in the *Df(16)A*$^{+/-}$*;Mirta22*$^{+/-}$ mice, compared with WT littermates. The number of days needed to reach criterion in the WM task did not differ significantly between *Df(16)A*$^{+/-}$*;Mirta22*$^{+/-}$ mice and WT littermates, indicating a major improvement in their learning strategy [*Df(16)A*$^{+/-}$*;Mirta22*$^{+/-}$ vs. WT, post hoc Bonferroni comparisons; $P > 0.05$]. Consistently, *Df(16)A*$^{+/-}$*;Mirta22*$^{+/-}$ mice required significantly less training to reach the criterion compared with *Df(16)A*$^{+/-}$ mice [main genotype effect on acquisition time $F(3, 57) = 7.580$, $P < 0.001$, post hoc Bonferroni test, $P = 0.008$; Fig. 1*B*]. In fact, similar to WT littermates, the majority (~70%) of the *Df(16)A*$^{+/-}$*;Mirta22*$^{+/-}$ mice were able to learn the WM-dependent task by 3 d, compared with only 28% of the *Df(16)A*$^{+/-}$ mice (*SI Appendix*, Fig. S3*B*). A day-to-day performance analysis showed that *Df(16)A*$^{+/-}$*;Mirta22*$^{+/-}$ mice started from the same performance level as *Df(16)A*$^{+/-}$ mice, but they benefited more from training and reached the learning criterion at the same pace as their WT littermates (*SI Appendix*, Fig. S3*C*). Notably, similarly to PPI findings, *Mirta22*$^{+/-}$ mice were indistinguishable from WT mice in their WM learning performance (*SI Appendix*, Fig. S3*A*).

Deficits in social cognition represent another core symptom of SCZ psychopathology and a reliable predictor of functional outcome in patients (31, 32). Although rodents do not display all features of human social cognition, and comparable information on cross-species circuit recruitment is scarce, use of rodent tasks that evaluate social cognition (33) can serve as a useful proxy of the human condition. By using a SM task for mice (34), we recently showed that *Df(16)A*$^{+/-}$ mice display a markedly impaired SM (35). We used this task to test the effects of *Mirta22* reduction on SM. Our results show that the SM deficit of the *Df(16)A*$^{+/-}$ mice is reversed in the *Df(16)A*$^{+/-}$*;Mirta22*$^{+/-}$ mice. Upon reintroduction of a familiar juvenile mouse (Fig. 1*C*), *Df(16)A*$^{+/-}$*;Mirta22*$^{+/-}$ mice showed a strong reduction in social interaction, indicative of intact SM, comparable to WT and *Mirta22*$^{+/-}$ littermates [RM ANOVA, trial*genotype interaction $F(3, 60) = 7.264$, $P < 0.0001$]. As previously reported, *Df(16)A*$^{+/-}$ mice showed a sustained high interaction time [one-way ANOVA for trial 2, $F(3, 60) = 2.984$, $P = 0.038$; post hoc Bonferroni comparison WT vs. *Df(16)A*$^{+/-}$, $P = 0.05$]. The intact SM of the *Df(16)A*$^{+/-}$*;Mirta22*$^{+/-}$ mice was further evident by the difference score (Fig. 1*D*), which was fully restored to the WT levels [one-way ANOVA $F(3, 60)=7.264$, $P < 0.0001$; post hoc

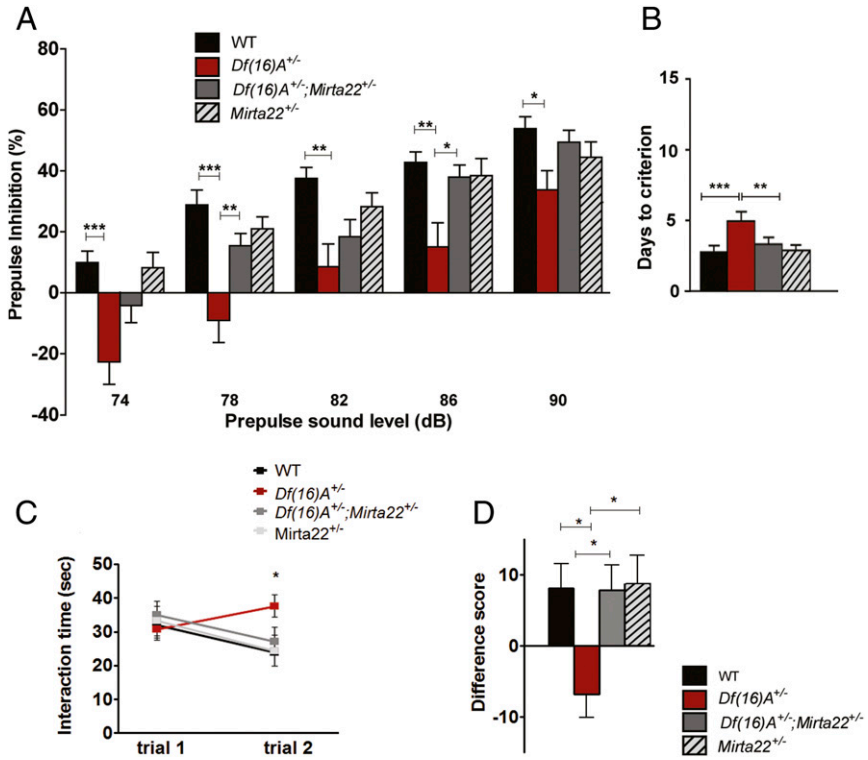

Fig. 1. *Mirta22* down-regulation rescues PPI, WM, and SM deficits in *Df(16)A*$^{+/-}$ mice. (*A*) Prevention of the sensorimotor gating impairment in the *Df(16)A*$^{+/-}$*;Mirta22*$^{+/-}$ mice compared with *Df(16)A*$^{+/-}$ littermates in particular for prepulse 78 db ($P = 0.007$) and 86 db ($P = 0.021$), as assayed by the PPI test. Percent PPI was calculated as 100 − [(startle response of acoustic startle from acoustic prepulse and startle stimulus trials/startle response alone trials) × 100]. $n = 16$ for *Df(16)A*$^{+/-}$*;Mirta22*$^{+/-}$; $n = 14$ for *Mirta22*$^{+/-}$ mice; $n = 13$ for *Df(16)A*$^{+/-}$; and $n = 17$ for WT. (*B*) Prevention of spatial WM impairment in the *Df(16)A*$^{+/-}$*;Mirta22*$^{+/-}$ mice, which show improved acquisition of the WM test (days to criterion) compared with *Df(16)A*$^{+/-}$ The vertical axis starts at 50% correct responses, which represents baseline accuracy expected by chance. Criterion was defined as the average choice accuracy during a training period, where the training endpoint was defined as two consecutive days of 70% choice accuracy or greater. $n = 16$ for *Df(16)A*$^{+/-}$*;Mirta22*$^{+/-}$; $n = 14$ for *Mirta22*$^{+/-}$ mice; $n = 13$ for *Df(16)A*$^{+/-}$; and $n = 17$ for WT. (*C* and *D*) Mirta22 down-regulation improves social memory deficit in the *Df(16)A*$^{+/-}$ mice. (*C*) Decrement in social investigation on trial 2 indicates social memory in the WT and the *Df(16)A*$^{+/-}$*;Mirta22*$^{+/-}$ mice, which is not the case for the *Df(16)A*$^{+/-}$ mice [RM ANOVA for genotype × trial, $F(3, 61) = 4.910$, $P = 004$]. (*D*) The negative difference score of the *Df(16)A*$^{+/-}$ mice [$F(3, 64) = 4.910$, $P = 004$, post hoc Bonferroni vs. WT, $P = 0.017$] indicates that these mice show no social memory. *Df(16)A*$^{+/-}$*;Mirta22*$^{+/-}$ mice show full restoration of difference SM score [post hoc Bonferroni vs. WT, $P = 0.1$, vs. *Df(16)A*$^{+/-}$, $P = 0.023$]. Data are presented as mean ± SEM. *$P < 0.05$; **$P < 0.01$; ***$P < 0.001$.

Bonferroni comparisons: *Df(16)A*$^{+/-}$ vs. WT $P = 0.002$, vs. *Df(16)A*$^{+/-}$*;Mirta22*$^{+/-}$, $P = 0.003$ vs. *Mirta22*$^{+/-}$, $P = 0.003$; *Df(16)A*$^{+/-}$*;Mirta22*$^{+/-}$ vs. WT, $P = 1.000$]. In conclusion, disruption in social cognition, along with disruptions in sensorimotor gating and WM, is linked to *Mirta22* derepression in the 22q11.2 mouse model of SCZ and is rescued by normalization of *Mirta22* levels.

Normalization of Mirta22 Levels Fails to Rescue Hyperactivity and Fear Memory Deficits. Hyperactivity in response to stress or novelty is widely used as a correlate of positive symptoms of SCZ in rodents, based on the notion that it could bear face validity for psychomotor agitation (36, 37). *Df(16)A*$^{+/-}$ mice are hyperactive compared with WT littermates, shown by total path length traveled over a 1-h exposure period and hyperactivity on a subsequent 30-min reexposure 24 h later (12). In the present study, *Df(16)A*$^{+/-}$ mice were found reproducibly hyperactive compared with WT mice (post hoc Bonferroni comparisons, day 1, $P < 0.0001$; day 2, $P = 0.013$) (Fig. 2*A*, day 1, and Fig. 2*B*, day 2). When Mirta22 levels were down-regulated in the compound *Df(16)A*$^{+/-}$*;Mirta22*$^{+/-}$ strain, hyperactivity in the open field (OF) was not affected during the initial 1-h exposure period [one-way ANOVA, main effect of genotype $F(3, 58) = 10.035$, $P < 0.0001$, post hoc Bonferroni comparison *Df(16)A*$^{+/-}$*;Mirta22*$^{+/-}$ vs. WT, $P = 0.007$] and only slightly reduced upon the 30-min reexposure 24 h later [one-way ANOVA, main effect of genotype $F(3, 58) = 4.378$, $P = 0.005$, post hoc Bonferroni comparison *Df(16)A*$^{+/-}$*;Mirta22*$^{+/-}$ vs. WT, $P = 0.099$]. *Mirta22*$^{+/-}$ mice showed levels of activity comparable to the WT mice. Moreover, analysis on center to margin measures did not reveal any preventive effect of Mirta22 down-regulation on state anxiety and fearful responses to novelty (Fig. 2 *A* and *B* and *SI Appendix*, Fig. S4*A*). Additional testing in the elevated plus maze did not reveal significant differences among genotypes in the time spent in the open arms (*SI Appendix*, Fig. S4*B*), suggesting that the "anxiety-like" phenotypes in *Df(16)A*$^{+/-}$ mice are task-specific (38, 39) and not directly affected by elevation of *Mirta22* levels.

A marked deficit in contextual and cued fear memory is one of the most reproducible and reliable phenotypes observed in *Df(16)A*$^{+/-}$ mice (12). This deficit likely reflects a readout of dysfunction in the neural circuit consisting of hippocampus (HPC), amygdala, and medial PFC (mPFC), all of which are involved in the learning and memory processes that promote adaptive context-dependent behavior (40, 41), but whose relation to increased SCZ risk remains tenuous. We have previously shown that the fear memory deficit cannot be accounted for fully by global miRNA dysregulation in *Dgcr8*-deficient mice (12). By subjecting mice to a fear-conditioning paradigm, we confirmed the fear memory deficit of the *Df(16)A*$^{+/-}$ mice compared with WT mice, both in contextual [one-way ANOVA $F(3, 61) = 3.128$, $P = 0.032$, post hoc Bonferroni comparisons, $P = 0.028$] and in cued fear memory [one-way ANOVA $F(3, 47) = 4.249$, $P = 0.010$,

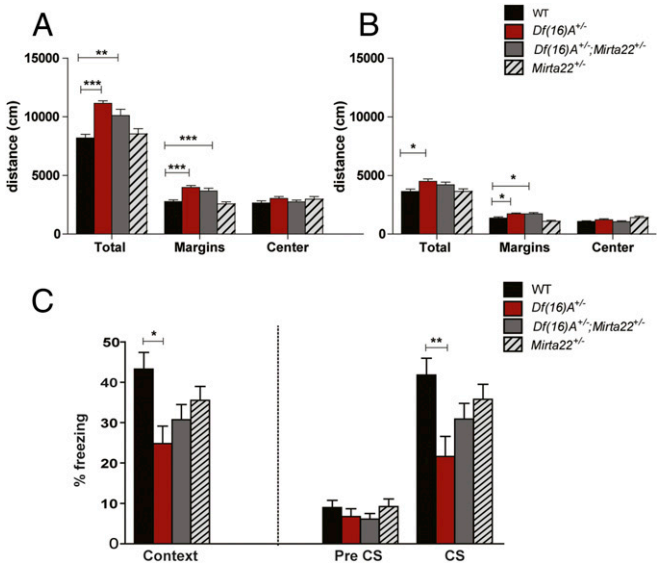

Fig. 2. *Mirta22* down-regulation does not rescue hyperactivity or fear memory in *Df(16)A*$^{+/-}$ mice. (*A* and *B*) Lack of rescue of hyperactivity in the OF on two consecutive days. In a 1-h exposure to a novel OF (*A*, day 1) *Df(16)A*$^{+/-}$; *Mirta22*$^{+/-}$ mice remain as hyperactive as *Df(16)A*$^{+/-}$ mice compared with WT ($P = 0.007$) and to a lesser extent during a 30-min reexposure 24 h later (*B*, day 2; ns). Similar to *Df(16)A*$^{+/-}$ mice, total distance traveled in the margin of the OF was significantly different for *Df(16)A*$^{+/-}$;*Mirta22*$^{+/-}$ mice, compared with WT (day 1, $P = 0.005$; day 2, $P = 0.042$), an indication that they were more fearful of exploring the novel environment (day 1: *Df(16)A*$^{+/-}$ vs. WT, $P < 0.0001$, *Df(16)A*$^{+/-}$ vs. *Mirta22*$^{+/-}$, $P < 0.0001$; day 2: *Df(16)A*$^{+/-}$ vs. WT, $P = 0.049$, *Df(16)A*$^{+/-}$ vs. *Mirta22*$^{+/-}$, $P < 0.001$). $n = 16$ for *Df(16)A*$^{+/-}$;*Mirta22*$^{+/-}$; $n = 14$ for *Mirta22*$^{+/-}$ mice; $n = 13$ for *Df(16)A*$^{+/-}$; and $n = 17$ for WT. (*C*) Deficits in fear conditioning test are not fully prevented. Twenty-four hours after exposure to the tone and foot-shock pairings, *Df(16)A*$^{+/-}$ mice showed significantly reduced freezing compared with WT mice when placed in the same context. Two hours after exposure to the contextual chamber, mice were placed into a novel chamber (PreCS), where mice of all genotypes only exhibited minimal freezing. When presented with the tone (CS), *Df(16)A*$^{+/-}$ mice froze significantly less than WT mice. $n = 16$ for *Df(16)A*$^{+/-}$;*Mirta22*$^{+/-}$; $n = 19$ for *Mirta22*$^{+/-}$ mice; $n = 12$ for *Df(16)A*$^{+/-}$; and $n = 13$ for WT. Data are presented as mean ± SEM. *$P < 0.05$; **$P < 0.01$; ***$P < 0.001$.

post hoc Bonferroni comparisons, $P = 0.014$] (Fig. 2*C*). Because there were neither increased baseline and postshock freezing levels nor differences in pain sensitivity (*SI Appendix*, Fig. S5*A*), these effects can only be attributed to fear memory impairment in the *Df(16)A*$^{+/-}$ mice. Consistent with our earlier findings in *Dgcr8*-deficient mice (12), reduction of Mirta22 levels in *Df(16)A*$^{+/-}$; *Mirta22*$^{+/-}$ mice was not sufficient to rescue deficits in either contextual or cued fear memory [no post hoc significant effects between *Df(16)A*$^{+/-}$;*Mirta22*$^{+/-}$ mice and *Df(16)A*$^{+/-}$ mice; Fig. 2*C*]. However, there was a small improvement in fear memory of *Df(16)A*$^{+/-}$;*Mirta22*$^{+/-}$ mice, because these mice do not differ significantly from their WT littermates. *Mirta22*$^{+/-}$ mice also demonstrated normal fear memory (Fig. 2*C*). This result suggests that Mirta22 normalization, in brain areas known to modulate fear memory, such as PFC and amygdala (*SI Appendix*, Fig. S1), is not on its own sufficient to fully rescue contextual and cued fear memory deficits in *Df(16)A*$^{+/-}$ mice.

Mirta22 Deficiency and Overexpression Have Dissociable Effects on Cognition and Behavior. Presence of a *Mirta22* LoF allele rescued specifically three SCZ-related behavioral impairments in *Df(16)A*$^{+/-}$ *mice* without evident widespread effects in other behavioral domains. This pattern of behavioral rescue may reflect simply a general essential role of *Mirta22* in modulating a subset of behaviors. Alternatively, it may reflect a more complex effect of Mirta22 elevated levels and inhibitory influences on behavioral outcomes, dissociating the effects of *Mirta22* up-regulation from those of down-regulation of its expression. The former simpler scenario would predict that complete LoF of *Mirta22* in a *Mirta22* knockout mouse model would result in alterations primarily in PPI, WM, and SM, but not in locomotor activity or associative fear memory. Surprisingly, our analysis of these behaviors in *Mirta22* knockout mice indicated that depletion of Mirta22 has the exact opposite effect.

Specifically, our analysis of *Mirta22*$^{-/-}$ mice and WT littermates showed no alterations in PPI, WM, or SM as a result of Mirta22 depletion (Fig. 3). This finding strongly suggests that altered PPI, WM, and SM in the *Df(16)A*$^{+/-}$ mice is directly linked to the elevation of Mirta22 levels above a permissive threshold indicated by the low physiological levels normally present in the postnatal brain.

Analysis of locomotor activity revealed that *Mirta22*$^{-/-}$ mice traveled far less total distance compared with WT in the 1 h of OF testing on day 1 ($P < 0.0001$) and upon 30-min reexposure on day 2 ($P < 0.0001$) (Fig. 4*A*). Notably, *Mirta22*$^{-/-}$ mice showed a significant increase in locomotor habituation occurring 20 min after the beginning of OF testing on day 1, but unaltered activity levels up to that point [Fig. 2*B*; RM ANOVA, genotype by time interaction $F(59; 1,180) = 1.612$, $P = 0.003$; genotype effect after 20 min, $P = 0.018$]. This enhanced locomotor habituation accounts for the decrease in total distance traveled by the *Mirta22*$^{-/-}$ mice. Interestingly, analysis of locomotor habituation of both *Df(16)A*$^{+/-}$ mice and *Df(16)A*$^{+/-}$;*Mirta22*$^{+/-}$ mice showed that they exhibited locomotor habituation comparable to the WT mice (Fig. 2*C*; RM

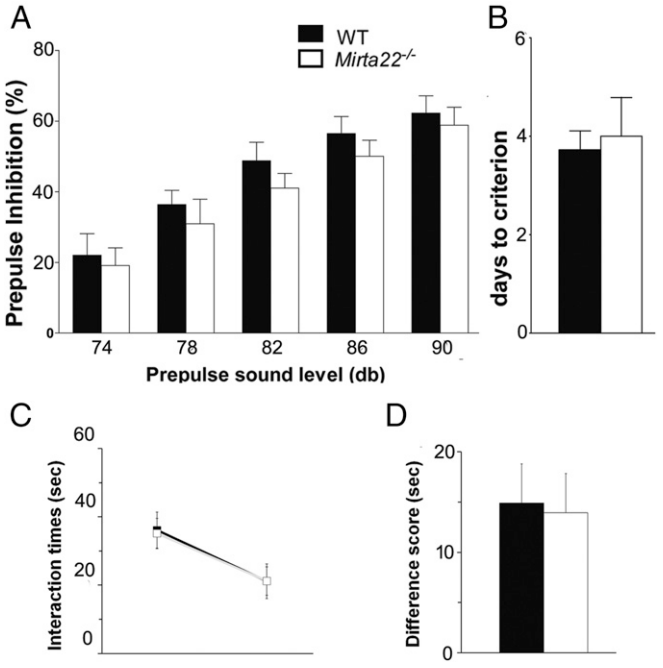

Fig. 3. Distinct effects of *Mirta22* deficiency on cognition and behavior: no effect on PPI, WM, and SM. (*A*) PPI test. *Mirta22*$^{-/-}$ mice do not show any significant differences in sensorimotor gating as assessed with PPI, compared with WT littermates. No significant genotype * PPI, WT vs. *Mirta22*$^{-/-}$, $P > 0.05$. (*B*) Spatial WM-dependent learning test. No differences were found in days to criterion between *Mirta22*$^{-/-}$ and WT ($P > 0.05$), suggesting that *Mirta22*$^{-/-}$ mice were comparably efficient in learning the spatial WM T-maze task. (*C* and *D*) Mirta22 deficiency does not affect SM. (*C*) Decrement in social investigation on trial 2 indicates normal SM in both the WT and the *Mirta22*$^{-/-}$ mice (RM ANOVA, no significant genotype × trial interaction). (*D*) Intact SM indicated by the difference score (*t* test, WT vs. *Mirta22*$^{-/-}$, ns). Data are presented as mean ± SEM. *$P < 0.05$; **$P < 0.01$; ***$P < 0.001$.

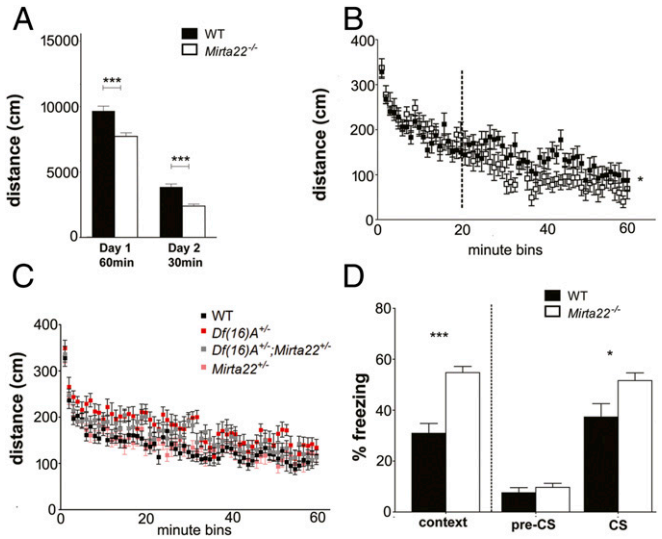

Fig. 4. Distinct effects of *Mirta22* deficiency on cognition and behavior: effects on locomotor habituation and fear memory. (*A*) OF test. *Mirta22*$^{-/-}$ mice showed an overall decrease in total distance on the initial 60-min exposure in the OF chamber (day 1), as well as upon a 30-min reexposure 24 h later (day 2). (*B*) Motor habituation in the OF. *Mirta22*$^{-/-}$ mice showed significantly enhanced locomotor habituation during the final 30 min of their initial OF exposure (day 1), as they gradually decreased the distance traveled at a higher degree compared with WT mice [RM ANOVA, genotype by time interaction $F(59; 1{,}180) = 1.612$, $P = 0.003$; genotype effect after 20 min $P = 0.018$]. (*C*) Motor habituation in the *Df(16)A*$^{+/-}$*;Mirta22*$^{+/-}$ mice. There were no significant differences on locomotor habituation in the *Df(16)A*$^{+/-}$*; Mirta22*$^{+/-}$ mice (RM ANOVA, no significant genotype by time interaction) suggesting that hyperactivity in these mice can be dissociated from the *Mirta22*-dependent effect on habituation. (*D*) Fear conditioning test. *Mirta22*$^{-/-}$ mice showed increased freezing both during reexposure to the conditioning context [$F(1, 20) = 24{,}015$; $P = 0.0001$] and during presentation of the CS [$F(1, 20) = 5{,}160$; $P = 0.035$]. Data are presented as mean ± SEM. $^{*}P < 0.05$; $^{**}P < 0.01$; $^{***}P < 0.001$.

ANOVA, no significant genotype by time interaction), although they started and remained hyperactive most of the time during their initial 1-h exposure to OF (main genotype effect vs. WT, $P = 0.009$). Thus, hyperactivity in *Df(16)A*$^{+/-}$ and *Df(16)A*$^{+/-}$*;Mirta22*$^{+/-}$ mice did not seem to be due to inability to habituate in a novel environment. This finding indicates that Mirta22 levels modulate locomotor habituation, a simple form of nonassociative learning (42–44), rather than activity per se, explaining at least in part the inefficiency of Mirta22 down-regulation to rescue hyperactivity of the *Df(16)A*$^{+/-}$ mice.

We also subjected *Mirta22*$^{-/-}$ mice and their WT littermates to a fear-conditioning paradigm. WT freezing levels for contextual fear memory were somewhat lower than the ones observed in the same assay on *Df(16)A*$^{+/-}$ mice and their WT littermates (Fig. 2*C*), but within the range reported in the literature (e.g., refs. 45 and 46). This result is likely due to differences in backcrossing generations (*Materials and Methods*), as well as differences in home cage microenvironment (47–49) that should similarly affect both genotypes. Analysis of fear learning revealed a marked effect of Mirta22 deficiency on associative memory, in which *Mirta22*$^{-/-}$ mice showed enhanced fear memory as expressed with higher freezing levels, both in the contextual version of fear memory recall [$F(1, 20) = 24{,}015$; $P = 0.0001$] and in the cued [$F(1, 20) = 5{,}160$; $P = 0.035$] (Fig. 4*D*). Mirta22 deficiency was not associated with increased baseline or postshock freezing levels, suggesting that any observed effects are specific to memory and not associated with increased anxiety or pain levels in the *Mirta22*$^{-/-}$ mice, as verified with a pain sensitivity test (*SI Appendix*, Fig. S5*B*). Also, freezing levels before presentation of the cue, during memory recall, were similar between *Mirta22*$^{-/-}$ mice and their WT littermates, ruling out fear overgeneralization and pointing to the specificity of the cue memory. This result reveals a strong negative association between Mirta22 levels and associative fear memory. In that respect, the inability of *Mirta22* down-regulation to fully prevent fear memory deficits in the *Df(16)A*$^{+/-}$ mice is quite surprising and likely points to a complicated interaction between Mirta22 overexpression and other genes removed by the 22q11.2 microdeletion, which results in rather intractable alterations in the neural circuits controlling fear learning. Interestingly, novel object recognition memory did not differ between WT and *Mirta22*$^{-/-}$ mice (*SI Appendix*, Fig. S6), which was also unaffected in the *Df(16)A*$^{+/-}$ mice (16), pointing to the selectivity and specificity of altered Mirta22 expression on cognition.

Despite pointing to dissociable effects of up-regulation vs. down-regulation of Mirta22, together, our behavioral findings described above suggest that Mirta22 down-regulation, depending on the testing context and the overall genetic makeup, facilitates specific cognitive processes, such as WM, habituation to novelty, and associative emotional learning.

Reduction of Mirta22 Levels in Df(16)A$^{+/-}$ Mice Rescues Synaptic Plasticity in the mPFC. Many of the cognitive processes supported by the PFC and the accompanying complex processing of multimodal information have been linked to local alterations of synaptic plasticity (50, 51). Short-term depression (STD), as well as both short-term potentiation (STP) and long-term potentiation (LTP), has been linked to processing of sensory information, WM, decision making, and other PFC-dependent cognitive processes (52–54). Altered synaptic plasticity in the PFC underlies various neuropsychiatric disorders, including SCZ, and has been linked to various endophenotypes, including primarily WM impairments, but also sensorimotor gating and social cognition deficits (50, 55, 56). Because the *Df(16)A*$^{+/-}$ *mice* are both impaired in PFC-dependent behaviors and display robust changes in PFC synaptic plasticity [as opposed to hippocampal synaptic plasticity (57)], they provide an ideal tool to examine whether reduction of Mirta22 levels in *Df(16)A*$^{+/-}$ mice also rescues PFC synaptic plasticity. To this end, we performed a series of PFC synaptic assays on *Df(16)A*$^{+/-}$, WT, and *Df(16)A*$^{+/-}$*; Mirta22*$^{+/-}$ mice. Guided by our behavioral analysis that consistently showed normal performance in all three SCZ-related assays, *Mirta22*$^{+/-}$ and *Mirta22*$^{-/-}$ mice were not included in this analysis.

It has been shown that older (16–20 wk old), but not younger (4–6 wk old) (15), *Df(16)A*$^{+/-}$ mice show a decrease in layer 5 (L5) field excitatory postsynaptic potentials (fEPSPs) upon direct stimulation of L2 neurons with increasing stimulation intensities. Our results corroborated this deficit. At higher stimulation intensities, the evoked fEPSPs were smaller in the *Df(16)A*$^{+/-}$ mice, but this deficit was rescued in *Df(16)A*$^{+/-}$*;Mirta22*$^{+/-}$ mice [Fig. 5*A*, input–output curve; two-way RM ANOVA, intensity by genotype interaction, $P < 0.001$; main effect of genotype, $P = 0.037$; post hoc Bonferroni *Df(16)A*$^{+/-}$*;Mirta22*$^{+/-}$ vs. *Df(16)A*$^{+/-}$, $P = 0.036$; *Df(16)A*$^{+/-}$*;Mirta22*$^{+/-}$ vs. WT, $P = 1$]. Given that fEPSPs obtained by using paired-pulse stimulation were not different among genotypes (*SI Appendix*, Fig. S7), the differences in synaptic strength at higher stimulation intensities could not be attributed to differences in the probability of neurotransmitter release at the L2–5 synapses. This result suggests that the rescue of fEPSP slopes in *Df(16)A*$^{+/-}$*;Mirta22*$^{+/-}$ mice may arise from reinstatement of the number of functional synapses due to the normalization of spine density in L5 neurons (see below).

Df(16)A$^{+/-}$ mice also exhibit significantly higher fEPSP STD at high train stimulation, but normal neurotransmitter release, as assessed by a paired-pulse facilitation (PPF) protocol (16). Here, we corroborated consistent deficits at 50 Hz, but we did not detect any difference between genotypes at lower (5 and 20 Hz) stimulation intensities (*SI Appendix*, Fig. S7*C*). At 50 Hz [Fig. 5*B*; WT,

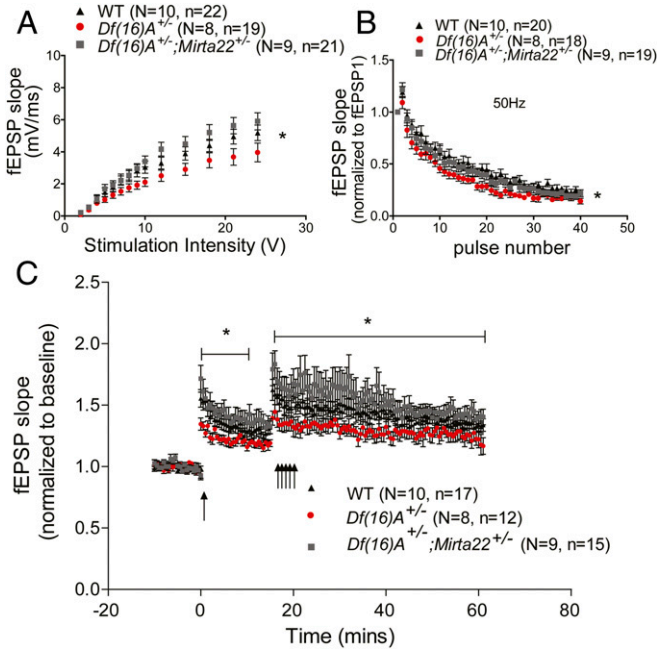

Fig. 5. *Mirta22* down-regulation rescues synaptic plasticity changes. (*A*) Plot showing stimulus–response curve across experiments (two-way RM ANOVA, stimulus by genotype interaction, $P < 0.0001$; genotype effect, $P = 0.037$). (*B*) STD at 50 Hz is rescued in the $Df(16)A^{+/-};Mirta22^{+/-}$ mice [two-way RM ANOVA, main effect of genotype, $P = 0.003$; post hoc Bonferroni, $P = 0.035$ vs. $Df(16)A^{+/-}$, $P = 1$ vs. WT]. (C) Plot showing synaptic potentiation in WT (black triangles), $Df(16)A^{+/-}$ (red circles), and $Df(16)A^{+/-};Mirta22^{+/-}$ (gray squares) mice. There is a significant difference in the degree of STP and LTP of fEPSPs over time (two-way RM ANOVA, $P = 0.024$ for STP and $P = 0.050$ for LTP). At the end of the first 50-Hz train (first arrow), the level of STP is rescued in the $Df(16)A^{+/-};Mirta22^{+/-}$ mice [$Df(16)A^{+/-};Mirta22^{+/-}$ vs. $Df(16)A^{+/-}$ post hoc test, $P = 0.02$]. Similarly, after the four consecutive 50-Hz trains (four arrows), the normalization in potentiation for the $Df(16)A^{+/-};Mirta22^{+/-}$ mice lasts for the entire duration of the remaining testing period [$Df(16)A^{+/-};Mirta22^{+/-}$ vs. $Df(16)A^{+/-}$ post hoc test, $P = 0.045$]. Values are normalized to slope of the first fEPSP in the train (*B*) or to the baseline (*C*). $Df(16)A^{+/-};Mirta22^{+/-}$ ($n = 9$), $Df(16)A^{+/-}$ ($n = 8$), and WT ($n = 10$). Data are presented as mean ± SEM. $*P < 0.05$; $**P < 0.01$; $***P < 0.001$.

$n = 10$, $n = 18$; $Df(16)A^{+/-}$, $n = 8$, $n = 15$; $Df(16)A^{+/-};Mirta22^{+/-}$ $n = 9$, $n = 17$], the observed initial facilitation between the first two pulses of the 50-Hz train was followed by a STD of the fEPSPs. In agreement with previous observations (16), STD was significantly enhanced in the $Df(16)A^{+/-}$ mice (two-way RM ANOVA, main effect of pulse number, $P < 0.0001$; significant effect of genotype $P = 0.003$; Bonferroni post hoc comparison vs. WT, $P = 0.003$). Down-regulation of Mirta22 expression resulted in a full rescue of STD in the $Df(16)A^{+/-};Mirta22^{+/-}$ mice (Fig. 5*B*; Bonferroni post hoc comparison vs. WT, $P = 1.000$, vs. $Df(16)A^{+/-}$, $P = 0.035$).

We also induced STP and LTP in acute PFC slices as described (16). STP was defined as a decremental potentiation lasting 10–30 min (58, 59), whereas LTP represents the non-decremental potentiation. After a stable 10- to 15-min baseline, a 50-Hz stimulation train was applied to L2 to induce STP in L5 of the mPFC, monitored every 30 s for 15 min. In agreement with earlier reports (16), $Df(16)A^{+/-}$ mice showed a marked deficit in STP compared with WT littermates (Fig. 5*C*; RM ANOVA, main effect of time, $P < 0.0001$; main effect of genotype, $P = 0.024$; post hoc comparison, $P = 0.062$). Restoring normal Mirta22 expression levels in $Df(16)A^{+/-};Mirta22^{+/-}$ mice resulted in reinstating STP responses in $Df(16)A^{+/-};Mirta22^{+/-}$ mice that were indistinguishable from WT mice ($P = 0.734$) and significantly improved compared with $Df(16)A^{+/-}$ mice ($P = 0.002$). At the end of the 15-min period, we induced LTP by applying four trains of 50 Hz separated by 10 s and monitored the fEPSP slopes for 40 min after the tetanic stimulation. In agreement with our previous results, potentiation was significantly reduced in $Df(16)A^{+/-}$ mice (Fig. 5*C*; two-way RM ANOVA, time × genotype interaction, $P < 0.0001$; main effect of genotype, $P = 0.05$). LTP responses of $Df(16)A^{+/-};Mirta22^{+/-}$ mice were rescued to WT levels ($P = 0.559$) and significantly improved compared with $Df(16)A^{+/-}$ mice (post hoc Bonferroni comparisons, $P = 0.044$).

Overall, considering the central role that PFC synaptic plasticity plays in maintaining WM, the modulatory role that PFC has on sensorimotor gating, and the remarkable effect of Mirta22 reduction in preventing PFC synaptic plasticity alterations, it is tempting to speculate that the effect of Mirta22 normalization on improving synaptic plasticity deficits in the PFC contributes to the rescue of the PPI and WM deficits.

Reduction of Mirta22 Levels Prevents Structural Alterations in the mPFC of $Df(16)A^{+/-}$ Mice. Given the effectiveness of Mirta22 down-regulation in preventing PFC synaptic plasticity deficits and our reported findings that normalization of Mirta22 expression prevents the emergence of structural alterations in CA1 hippocampal neurons (14), we asked whether such function is extended to the PFC, potentially contributing to the observed improvements in synaptic plasticity (Fig. 6). To analyze spine and dendrite morphology in L5 neurons in the prelimbic area of mPFC, we crossed $Thy1\text{-}GFP^{+/-}$ mice with $Df(16)A^{+/-}$ and $Mirta22^{+/-}$ mice to generate $Df(16)A^{+/-};GFP^{+/-}$ and $Mirta22^{+/-};GFP^{+/-}$ mice, respectively. We then crossed $Df(16)A^{+/-};GFP^{+/-}$ with $Mirta22^{+/-};GFP^{+/-}$ mice to generate $Df(16)A^{+/-};GFP^{+/-}$, $Df(16)A^{+/-};Mirta22^{+/-};GFP^{+/-}$, and $WT/GFP^{+/-}$ littermates, which we used to assess basal dendrite morphology. This analysis confirmed previously reported structural abnormalities in terms of reduced spine density of $Df(16)A^{+/-}$ prelimbic pyramidal neurons. Notably, genetic removal of one copy of *Mirta22* is sufficient to prevent reductions of spine density [Fig. 6*D*; WT vs. $Df(16)A^{+/-}$, $P < 0.0001$; $Df(16)A^{+/-}$ vs. $Df(16)A^{+/-};Mirta22^{+/-}$, $P < 0.0001$] and width [Fig. 6*E*; WT vs. $Df(16)A^{+/-}$, $P < 0.0001$; $Df(16)A^{+/-}$ vs. $Df(16)A^{+/-};Mirta22^{+/-}$, $P < 0.0001$] in mushroom spines at the basal dendritic tree of L5 pyramidal neurons in the prelimbic area of mPFC, with all metrics comparable to WT levels [WT vs. $Df(16)A^{+/-}$;$Mirta22^{+/-}$, ns]. Similar reversal on spine density deficits were observed in different types of spines as well, namely, long and filopodium (*SI Appendix*, Fig. S8).

Discussion

We demonstrate that the presence of a LoF *Mirta22* allele in $Df(16)A^{+/-}$ mice, a mouse model of the SCZ-associated 22q11.2 microdeletion, where Mirta22 is up-regulated, is sufficient to prevent primary SCZ-related cognitive and behavioral deficits, along with underlying synaptic and structural plasticity alterations in the PFC. Because depletion of Mirta22 levels in *Mirta22* knockout mice did not result in abnormalities in any of these behavioral phenotypes, the observed rescue likely reflects prevention of the deleterious effects of Mirta22 up-regulation in the context of the 22q11.2 locus.

Our results also suggest that failure of Mirta22 expression to subside into physiological levels at early postnatal life due to genomic loss at the 22q11.2 locus could be causally linked to the initiation of a chain of events, which prohibits neuronal circuits from attaining the degree of connectivity and plasticity that is necessary to subserve cognitive and behavioral faculties. In that respect, our work provides a comprehensive model of the consequences of altered miRNA regulation in $Df(16)A^{+/-}$ mice, attributed to the failure to restrict and optimize postnatal *Mirta22* expression, a key breakdown in miRNA-dependent homeostatic regulation by the 22q11.2 genomic locus. This model is useful, offering a plausible synaptic and circuit explanation of

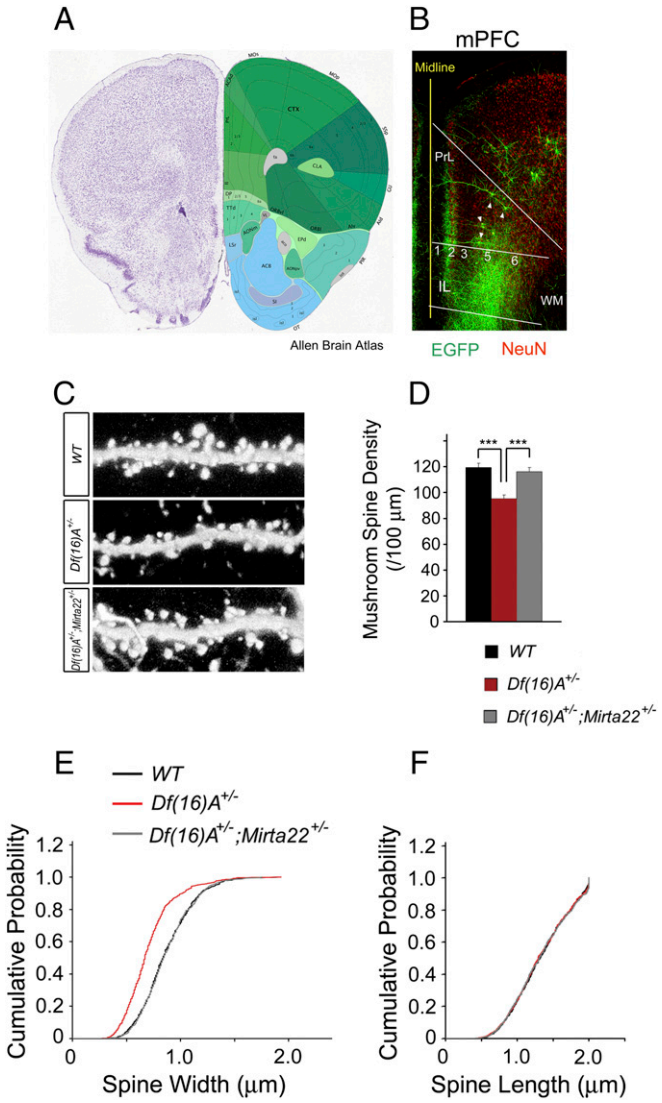

Fig. 6. *Mirta22* down-regulation rescues spine density and width in basal dendrites of L5 pyramidal neurons in prelimbic area of mPFC. (*A*) Representative image of Nissle stain (*Left*) and reference map (*Right*) of a coronal section in mPFC is from the Allen Brain Atlas. IL, infralimbic area; PrL, prelimbic area. (*B*) Representative image of EGFP-labeled neurons in L5 (arrowheads) in PrL of the *Thy1-GFP*$^{+/-}$;*Df(16)A*$^{+/-}$;*Mirta22*$^{+/-}$ mouse. Numbers indicate cortical layers. (*C*) Representative images of spines at basal dendrites of EGFP-expressing L5 neurons in the prelimbic area of mPFC. Brains were dissected from 8-wk-old littermate mice. (*D*) Reduction in the density of mushroom spines in *Df(16)A*$^{+/-}$ neurons at 8 wk relative to WT neurons is prevented in the *Df(16)A*$^{+/-}$;*Mirta22*$^{+/-}$ mice ($n = 6$ per genotype, $n = 24$ for all genotypes). (*E*) Width of mushroom spines in the basal dendritic tree of L5 pyramidal neurons in the prelimbic area of mPFC. Note that reduction in width is prevented in the *Df(16)A*$^{+/-}$;*Mirta22*$^{+/-}$ mice ($P < 0.0001$, Kolmogorov–Smirnov test). (*F*) Length of mushroom spines in the basal dendritic tree of L5 pyramidal neurons in the prelimbic area of mPFC. No genotypic differences were observed.

one facet of the 22q11 microdeletion syndrome by crossing boundaries between multiple levels of analysis, providing a framework for future studies, and importantly pointing to several possible avenues for therapeutic interventions.

Nonetheless, this model is still incomplete in its details. First, whether Mirta22 up-regulation impacts brain maturation during a critical stage of early postnatal synapse formation or whether abnormal sustained elevation of Mirta22 throughout the adult life interferes with ongoing synaptic communication and plasticity remains to be determined. Second, whether Mirta22 up-regulation affects additional SCZ-related behaviors as well as neural circuitry in other brain regions (35) remains unknown. Although our synaptic plasticity and morphological assays point to the PFC, as an underlying substrate for our behavioral findings, it is very likely that *Mirta22* up-regulation affects the fine structure and activity of other brain regions, including, for example, hippocampal area CA2, which plays a crucial role in social learning and is dysfunctional in *Df(16)A*$^{+/-}$ mice (27). Along the same lines, the neural basis of the specificity of behavioral rescue also remains unknown. Given that *Mirta22* is widely expressed in the brain (https://gtexportal.org/home/gene/EMC10; *SI Appendix*, Fig. S9) and its expression is similarly normalized in all three brain areas tested in *Df(16)A*$^{+/-}$;*Mirta22*$^{+/-}$ mice (*SI Appendix*, Fig. S1), this specificity is likely related to the way that the developmental pattern of Mirta22 expression is altered by the 22q11.2 miRNA dysregulation and how this alteration affects the postnatal maturation and function of brain areas subserving specific behavioral outputs. Third, our behavioral analysis used three cohorts of group-housed mice, with one of them subjected sequentially in three behavioral assays (*Materials and Methods*). Therefore, our behavioral findings should be interpreted in the context of the sequence and prior test history of the behavioral assays. However, all behaviors tested are robust and reproducible and have been previously observed in multiple cohorts independently of the testing history. Fourth, because only male mice were used in our analysis, it remains to be determined whether the beneficial effects of *Mirta22* reduction encompass both sexes. Finally, the exact molecular and cellular mechanisms by which derepression of Mirta22 contributes to abnormal neuronal, synaptic, and circuit maturation remain unknown. The striking effect of normalization of Mirta22 levels may be linked to a possible role of MIrta22 in the elimination of misfolded membrane proteins as part of endoplasmic reticulum-associated degradation complex (60). It may also be linked to a potential role of Mirta22 in membrane and protein trafficking and secretion related to its localization in Golgi apparatus and in vesicle and tubular-like extensions in dendrites and axons (14). This process is located in the core of maturation and maintenance of neuronal connections and physiological levels of synaptic plasticity (61, 62). It is also possible that, in its secreted form (63), Mirta22 interacts and interferes with neurotrophic or extracellular matrix factors known to mediate activity-dependent dendritic plasticity (64, 65).

Disease risk conferred by large pathogenic copy number variants (CNVs) is likely due to the action of multiple risk genes. This hypothesis has been suggested both by our early work in mouse models of the 22q11.2 deletion (15) and by more recent human genetic studies, which showed that large CNVs contain multiple modest-effect risk genes (66). Consistent with this view, *Mirta22* is likely to act in concert with other genes within the 22q11.2 deletion that modulate either distinct phenotypes (such as hyperactivity or fear learning) that were not rescued by reduction of Mirta22 or overlapping phenotypes rescued by Mirta22 reduction. In the latter case, one example is *Zdhhc8*, which is also located in the Golgi apparatus, and is involved in membrane trafficking of neuronal proteins. *Zdhhc8* deficiency affects some of the same behavioral (WM) and cellular phenotypes rescued by reduction of Mirta22 levels (67–69), in part by leading to hyperactive Gsk3 signaling and stunted growth of developing axonal terminals. Notably, we have recently shown that developmental inhibition of Gsk3 activity was also successful in rescuing WM and related neurophysiological deficits in the *Df(16)A*$^{+/-}$ mice (67, 69), pointing to more than one mechanism by which a pathogenic CNV affects a given behavior, as well as more than one entry point for therapeutic interventions.

Our findings also offer more general insights into the genetic and neural architecture of psychiatric and neurodevelopmental disorders, in particular in the feasibility of implementing protective-variant searches by exploiting data from well-characterized valid genetic disease models. A large number of relatively rare LoF variants that result in a nonfunctional or unstable gene product as well as potentially damaging missense variants have been identified in the human ortholog of *Mirta22* (*Emc10*) gene (exac.broadinstitute.org/gene/ENSG00000161671) (70). It is likely that such variants, when they cooccur with the 22q11.2 deletion, can confer protection against the risk, severity, or both of the 22q11.2-associated psychiatric and cognitive symptoms. Given the large numbers of affected 22q11.2 deletion carriers being required to generate sufficient discovery power, the resources required to test this prediction in humans are not currently available. It is also conceivable that other genetic lesions predisposing to SCZ also lead to up-regulation of Mirta22 activity or to aberrant repression of cellular processes where Mirta22 plays an important restraining role. The nature and prevalence of such mutations remains unknown, but it is plausible that impaired Mirta22 function may be beneficial in the context of additional mutations that predispose to psychiatric disorders. Along these lines, exploratory use of the sequence-kernel association test to test whether *MIRTA22* (*EMC10*) variants confer protective effects (and therefore are underrepresented) in a publicly available SCZ cohort of modest size (*SI Appendix*) revealed a significant difference between cases and controls, indicating the existence of a small protective effect of *MIRTA22* (*EMC10*) variants on SCZ risk. In support of this possibility, it was recently shown that 22q11.2 duplications, which result in reduced *Mirta22* levels (14), might exert a protective effect in general SCZ risk (71, 72). Again, given the considerable challenges in identifying rare protective LoF variants in common complex disorders such as SCZ, due to the rarity of these variants and the very large number of patients required (5), our results highlight the quintessential role that animal models may play in identifying such "advantageous" gene losses.

A major attraction of the inquiry for protective LoF variants is the potential for a novel therapeutic target roadmap. In that respect, the elucidation of the sequence of events that lead from the 22q11.2 deletion to cognitive and synaptic deficits, the demonstration that Mirta22 reduction can prevent emergence of some of these deficits, and the lack of any obvious adverse effects point to manipulation of Mirta22 expression as a potential treatment target. In that respect, it is remarkable that, unlike common antipsychotics, which ameliorate PPI but are minimally effective or completely ineffective in improving cognitive deficits, *Mirta22* level regulation has been successful in reversing both PPI and two core SCZ cognitive deficits, such as WM and SM deficits. Furthermore, the similar developmental pattern of Mirta22 expression between mice (14), humans (*SI Appendix*, Fig. S10; Allen Brain Institute), and nonhuman primates (*SI Appendix*, Fig. S11; Allen Brain Institute), with a strong prenatal bias and a gradual decrease in expression with age, suggests a conserved mechanism of action and directly links our results in mice to possible treatment strategies in humans. Along these lines, in future experiments, it is important to determine when during the lifespan Mirta22 normalization is most effective at reversing behavioral and neurophysiological phenotypes and whether Mirta22 levels could be normalized by approaches as readily translatable into medical therapies as possible. These approaches include, for example, the application of siRNAs or shRNAs (73, 74) or the use of antisense oligonucleotides to inhibit excessive *Mirta22* gene expression based on their efficacy in preclinical models (75, 76) and clinical studies (77, 78) of neurodevelopmental or neurodegenerative disorders. Alternatively, use of genome editing via CRISPR could be another highly promising approach for modulating *Mirta22* function (79, 80). Additionally, specific targeting of pathogenic or overexpressed forms of proteins has proven highly successful in cancer research and appears promising in the treatment of neurodegenerative disorders as well (81, 82). This method is of particular interest in the case of Mirta22, because a secreted form of the protein has been found both in vitro and in human serum (14, 63). Highly selective targeting of secreted Mirta22 in the brain (i.e., by monoclonal antibodies) could improve the behavioral and cognitive deficits associated with the 22q11.2 microdeletion. Furthermore, deciphering the function of Mirta22 and exploring its interactions with other neuronal molecular partners will provide insights into its specific role in neuronal processes and offer downstream targets for potential inhibition by specific pharmaceutical compounds. For such strategies to be successful, it will be important to determine the developmental window during which *Mirta22* expression manipulations could be efficacious, because the diagnosis of SCZ is rarely made before late adolescence. Restricting the overexpression of *Mirta22* in children carrying 22q11.2 deletions during early postnatal life will provide a framework for prevention, whereas its inhibition during adulthood could serve as an improved alternative or augmentation of current treatments because it might offer alleviation from cognitive deficits and psychotic symptoms.

If our findings eventually lead to novel treatments for the 22q11.2 deletion syndrome, it is unclear whether they will also apply to SCZ cases arising from other causes, given the high level of genetic heterogeneity of the disorder. The observation that Mirta22 down-regulation enhances specific aspects of cognitive functioning (i.e., novelty habituation and associative fear memory) even in a WT background, suggests that treatment interventions via inhibition of the product of this gene could be more generally applicable.

Overall, coupled with emerging ideas regarding beneficial LoF mutations, our results represent not only a decisive step toward a comprehensive understanding of the neurobiological consequences of the 22q11.2 deletions and the contribution of miRNA-dependent gene regulation to psychiatric and neurodevelopmental disorders, but also a decisive step toward translating these mechanistic insights into bona fide improvements in clinical management.

Materials and Methods

All procedures were conducted in accordance with NIH regulations and approved by Columbia University and New York State Psychiatric Institute Institutional Animal Care and Use Committees.

Mutant Mice. *Df(16)A*$^{+/-}$ mice have been described (12, 68) and have been backcrossed into C57BL/6J background for >10 generations. Mirta22 mutant mice [2310044H10RikGt(OST181617)Lex/Mmucd (referred to as *Mirta22*$^{+/-}$)] were obtained from the Mutant Mouse Regional Resource Centers supported by NIH and have been backcrossed into C57BL/6J background for over five generations. The compound heterozygote for Df(16)A and a Mirta22 knockout allele strain was generated by crossing *Df(16)A*$^{+/-}$ male mice with *Mirta22*$^{+/-}$ female mice of 8–12 wk of age. *Df(16)A*$^{+/-}$ × *Mirta22*$^{+/-}$ crossings produced the following four genotypes: (*i*) *Df(16)A*$^{+/-}$;*Mirta22*$^{+/-}$, (*ii*) *Df(16)A*$^{+/+}$;*Mirta22*$^{+/-}$ (these are referred to as *Mirta22*$^{+/-}$ for simplicity), (*iii*) *Df(16)A*$^{+/-}$;*Mirta22*$^{+/+}$ (these are referred to as *Df(16)A*$^{+/-}$), and (*iv*) *Df(16)A*$^{+/+}$;*Mirta22*$^{+/+}$ (these are referred to as WT). Male offspring of all four genotypes, as well as male *Mirta22*$^{-/-}$ and WT littermates, were used for behavioral testing. One cohort of mice was used for OF, PPI, and T-maze tasks, in that order; a separate cohort was used for SM assay; and a third cohort was used for the FC task. We also performed behavioral studies on three cohorts of *Mirta22*$^{-/-}$ and WT littermates in a similar way: one cohort of mice for OF, PPI, and T-maze tasks, in that order; a separate cohort for SM assay; and a third cohort for the FC task. Male mice of *Df(16)A*$^{+/-}$;*Mirta22*$^{+/-}$, *Df(16)A*$^{+/-}$, and WT genotypes were used for electrophysiological recordings, whereas both male and female *Df(16)A*$^{+/-}$;*Mirta22*$^{+/-}$, *Df(16)A*$^{+/-}$, and WT mice were used for cellular morphology analysis. Details on mouse numbers can be found in *SI Appendix*.

Behavioral Testing. Behavioral phenotyping was performed as described (12). Male mice at 8 wk of age at testing initiation were tested in open-field, PPI, and spatial WM (in that order). Two additional separate cohorts of mice were used for social memory and Pavlovian fear conditioning assays, respectively. Between-test intervals were 3 d after OF and before PPI and 1 wk after PPI and before T-maze. Although we left a week in between PPI testing and the beginning of the T-maze procedure, gene–environment interaction effects on WM performance cannot be excluded. However, several separate cohorts of *Df(16)A*$^{+/-}$ and WT mice have been tested for WM only in the laboratory, which consistently identified the same learning deficit for the *Df(16)A*$^{+/-}$ mice. Because the T-maze test for WM involves single housing, food restriction, and extensive experimenter handling, which cause stress on the animals, PPI was tested first to avoid influences of all these factors. All animal procedures performed were described in protocols approved by the Columbia University Institutional Animal Care and Use Committee under federal and state regulations. Details about behavioral assays can be found in *SI Appendix*.

Electrophysiology in mPFC Slice Preparations. Experiments were performed as described (16) on 16- to 20-wk-old mice that had undergone the fear-conditioning task. Results were in general in very good agreement with two previous studies using mice of the same (35) or younger (15) age. Differences observed compared with ref. 15 are likely attributed, at least in part, to age-dependent effects on synaptic transmission and plasticity. Isoflurane was used to anesthetize mice that were then decapitated. After a skull incision, the brain was removed and placed in ice-cold dissecting solution containing (in mM) 195 sucrose, 10 NaCl, 2.5 KCl, 1 NaH_2PO_4, 25 $NaHCO_3$, 10 glucose, 4 $MgSO_4$, and 0.5 $CaCl_2$. The cerebellum and part of the HPC were removed, and coronal brain sections were cut on a vibratome (Leica VT1200S). The freshly cut mPFC slices were immediately transferred to an interface chamber and allowed to recover for at least 2 h at 34–36 °C. During all recordings, the slices were continuously perfused with artificial CSF (aCSF) (bubbled with 5% CO_2/95% O_2) that had the following composition (in mM): 124 NaCl, 2.5 KCl, 1 NaH_2PO_4, 25 $NaHCO_3$, 10 glucose, 1 $MgSO_4$, and 2 $CaCl_2$. The aCSF was maintained at 34–36 °C and fed by gravity at a rate of 2–3 mL/min. fEPSPs were recorded via a glass microelectrode (3–5 MΩ) filled with aCSF and placed in L5 of the mPFC (600–700 μm from midline).The stimulation site was always aligned ∼200 μm away from the recording site along the axis perpendicular to the pial surface. Basic synaptic transmission was characterized at 0.033 Hz, with stimulation intensities of 3–24 V (pulse duration, 0.1 ms). The subsequent experiments were performed at the stimulus intensity that generated a fEPSP one-third of the maximum fEPSP obtained at 24 V. Short-term synaptic facilitation was induced by using a paired-pulse protocol with interspike intervals of 20, 50, 100, 400, and 800 ms. To assess STD, fEPSPs were evoked by using a 40-pulse train at 5, 20, and 50 Hz (pulse duration, 0.1 ms). LTP was induced by 40 pulses, 50-Hz train after a stable 10-min baseline, and monitored during 15 min. Then, 15 min after the first tetanus, four additional 50-Hz trains (separated by 10 s) were applied. The fEPSPs were then monitored for 40 min. Signals were acquired by using the pClamp10 software (Molecular Devices), the Digidata 1440A (Molecular Devices), and an extracellular amplifier (Cygnus Technologies). Fiber volley was quantified by measuring the amplitude of the first peak negativity of the field responses, and the fEPSPs were quantified by measuring the initial slope of the second peak negativity of the responses. Statistical analyses were performed by using the SigmaPlot and Statview software. Data are presented as means ± SEM. *N* indicates number of animals, and *n* indicates number of slices. All recordings and the majority of data analyses were performed blind to the genotype.

Image Analysis of Dendritic Spines. Image analysis was conducted blind to genotype as follows. For in vivo analysis, spine density and morphology measurements were conducted on Thy1-GFP$^{+/-}$ mice crossed with WT, *Df(16)A*$^{+/-}$, or *Df(16)A*$^{+/-}$*;Mirta22*$^{+/-}$. Df(16)A$^{+/-}$ mice were crossed to the Thy1–GFP/M mouse line. Adult male littermates, at 2–3 mo of age, were anesthetized and transcardially perfused with 1× PBS, followed by 4% PFA in PBS. Brains were postfixed in 4% PFA and then sectioned coronally at 100 μm on a vibratome (Leica). Sections were mounted and images were obtained on a Carl Zeiss LSM 510 laser-scanning confocal microscope. The cortical layers were identified by NeuN immunostaining and Nissl staining (Invitrogen), and the cortical thickness was divided into seven bins (bin 1, marginal zone and L1; bin 2, L2; bin 3, L3; bins 4 and 5, L5; and bins 6 and 7, L6). L5 pyramidal neurons were almost exclusively labeled in the mPFC of the mice, throughout the cell body and the dendritic tree. Z stacks were acquired at higher magnification to facilitate the measurement of spine number, size, and morphology. A region of interest encompassing a segment of >50 μm from the first branch point of the largest dendrite was defined in one or two of the largest dendrites of the neuron. The bent-line overlay tool of LSM Image Examiner 5 was used to measure the length of the spine from the surface of the dendritic shaft, including the neck and head of the spine. The straight-line tool was used to measure the width of the spine at its widest point. Dendritic protrusions were categorized as spines or filopodia and morphologically classified as mushroom, long, stubby, or thin by using parameters described in ref. 68. Specifically, spines with distinct heads were classified as "mushroom" if <2.0 μm or "long" if >2.0 μm. Spines without distinct heads were classified as "thin" if <2.0 μm or "stubby" if <1.0 μm but >0.35 μm. Protrusions without a distinct head and >2.0 μm were classified as filopodia.

Statistical Analysis. All behavioral and electrophysiology data were analyzed in SPSS with RM or one-way ANOVA with genotype as the factor and Bonferroni post hoc comparisons for the different genotypes. Data on the number, size, and shape of spines across conditions were analyzed with Student's *t* test, and the distribution of width of mushroom spines was compared by using the Kolmogorov–Smirnov test.

ACKNOWLEDGMENTS. We thank Pratibha Thakur for performing quantitative RT-PCR assays and assisting in behavioral experiments; Yan Sun, Caitlin Burgdorf, Rachel Waldman, and Naoko Haremaki for maintaining the mouse colony; and Iuliana Ionita-Laza for advising on genetic analysis. This work was supported by National Institute of Mental Health Grants MH097879 (to J.A.G.) and MH067068 (to M.K.).

1. Rodriguez-Murillo L, Gogos JA, Karayiorgou M (2012) The genetic architecture of schizophrenia: New mutations and emerging paradigms. *Annu Rev Med* 63:63–80.
2. Ayers KL, et al. (2016) A loss of function variant in CASP7 protects against Alzheimer's disease in homozygous APOE ε4 allele carriers. *BMC Genomics* 17:445–450.
3. Flannick J, et al.; Go-T2D Consortium; T2D-GENES Consortium (2014) Loss-of-function mutations in SLC30A8 protect against type 2 diabetes. *Nat Genet* 46:357–363.
4. Ding Q, et al. (2014) Permanent alteration of PCSK9 with in vivo CRISPR-Cas9 genome editing. *Circ Res* 115:488–492.
5. Harper AR, Nayee S, Topol EJ (2015) Protective alleles and modifier variants in human health and disease. *Nat Rev Genet* 16:689–701.
6. Langsted A, Nordestgaard BG, Benn M, Tybjærg-Hansen A, Kamstrup PR (2016) PCSK9 R46L loss-of-function mutation reduces lipoprotein(a), LDL cholesterol, and risk of aortic valve stenosis. *J Clin Endocrinol Metab* 101:3281–3287.
7. Lepor NE, Kereiakes DJ (2015) The PCSK9 inhibitors: A novel therapeutic target enters clinical practice. *Am Health Drug Benefits* 8:483–489.
8. Downes K, et al. (2010) Reduced expression of IFIH1 is protective for type 1 diabetes. *PLoS One* 5:e12646.
9. Hughes T, et al. (2016) A loss-of-function variant in a minor isoform of ANK3 protects against bipolar disorder and schizophrenia. *Biol Psychiatr* 80:323–330.
10. Levinson DF, et al. (2011) Copy number variants in schizophrenia: Confirmation of five previous findings and new evidence for 3q29 microdeletions and VIPR2 duplications. *Am J Psychiatry* 168:302–316.
11. International Schizophrenia Consortium (2008) Rare chromosomal deletions and duplications increase risk of schizophrenia. *Nature* 455:237–241.
12. Stark KL, et al. (2008) Altered brain microRNA biogenesis contributes to phenotypic deficits in a 22q11-deletion mouse model. *Nat Genet* 40:751–760.
13. Xu B, Karayiorgou M, Gogos JA (2010) MicroRNAs in psychiatric and neurodevelopmental disorders. *Brain Res* 1338:78–88.
14. Xu B, Hsu PK, Stark KL, Karayiorgou M, Gogos JA (2013) Derepression of a neuronal inhibitor due to miRNA dysregulation in a schizophrenia-related microdeletion. *Cell* 152:262–275.
15. Karayiorgou M, Simon TJ, Gogos JA (2010) 22q11.2 microdeletions: Linking DNA structural variation to brain dysfunction and schizophrenia. *Nat Rev Neurosci* 11:402–416.
16. Fénelon K, et al. (2013) The pattern of cortical dysfunction in a mouse model of a schizophrenia-related microdeletion. *J Neurosci* 33:14825–14839.
17. Fendt M, Li L, Yeomans JS (2001) Brain stem circuits mediating prepulse inhibition of the startle reflex. *Psychopharmacology (Berl)* 156:216–224.
18. Alsene KM, Rajbhandari AK, Ramaker MJ, Bakshi VP (2011) Discrete forebrain neuronal networks supporting noradrenergic regulation of sensorimotor gating. *Neuropsychopharmacol* 36:1003–1014.
19. Ellenbroek BA, Budde S, Cools AR (1996) Prepulse inhibition and latent inhibition: The role of dopamine in the medial prefrontal cortex. *Neuroscience* 75:535–542.
20. Japha K, Koch M (1999) Picrotoxin in the medial prefrontal cortex impairs sensorimotor gating in rats: Reversal by haloperidol. *Psychopharmacology (Berl)* 144:347–354.
21. Swerdlow NR, Geyer MA, Braff DL (2001) Neural circuit regulation of prepulse inhibition of startle in the rat: Current knowledge and future challenges. *Psychopharmacology (Berl)* 156:194–215.

22. Rabin RA, Sacco KA, George TP (2009) Correlation of prepulse inhibition and Wisconsin Card Sorting Test in schizophrenia and controls: Effects of smoking status. *Schizophr Res* 114:91–97.
23. Csomor PA, et al. (2008) Haloperidol differentially modulates prepulse inhibition and p50 suppression in healthy humans stratified for low and high gating levels. *Neuropsychopharmacol* 33:497–512.
24. Singer P, et al. (2013) Prepulse inhibition predicts working memory performance whilst startle habituation predicts spatial reference memory retention in C57BL/6 mice. *Behav Brain Res* 242:166–177.
25. Oliveras I, et al. (2015) Prepulse inhibition predicts spatial working memory performance in the inbred Roman high- and low-avoidance rats and in genetically heterogeneous NIH-HS rats: Relevance for studying pre-attentive and cognitive anomalies in schizophrenia. *Front Behav Neurosci* 9:213–229.
26. Wynn JK, Sergi MJ, Dawson ME, Schell AM, Green MF (2005) Sensorimotor gating, orienting and social perception in schizophrenia. *Schizophr Res* 73:319–325.
27. Mongillo G, Barak O, Tsodyks M (2008) Synaptic theory of working memory. *Science* 319:1543–1546.
28. Arguello PA, Gogos JA (2010) Cognition in mouse models of schizophrenia susceptibility genes. *Schizophr Bull* 36:289–300.
29. Funahashi S (2006) Prefrontal cortex and working memory processes. *Neuroscience* 139:251–261.
30. Sigurdsson T, Stark KL, Karayiorgou M, Gogos JA, Gordon JA (2010) Impaired hippocampal-prefrontal synchrony in a genetic mouse model of schizophrenia. *Nature* 464:763–767.
31. Green MF (2016) Impact of cognitive and social cognitive impairment on functional outcomes in patients with schizophrenia. *J Clin Psychiatry* 77:8–11.
32. Kalin M, et al. (2015) Social cognition, social competence, negative symptoms and social outcomes: Inter-relationships in people with schizophrenia. *J Psychiatr Res* 68: 254–260.
33. Ellenbroek BA, Cools AR (2000) Animal models for the negative symptoms of schizophrenia. *Behav Pharmacol* 11:223–233.
34. Kogan JH, Frankland PW, Silva AJ (2000) Long-term memory underlying hippocampus-dependent social recognition in mice. *Hippocampus* 10:47–56.
35. Piskorowski RA, et al. (2016) Age-dependent specific changes in area CA2 of the hippocampus and social memory deficit in a mouse model of the 22q11.2 deletion syndrome. *Neuron* 89:163–176.
36. Arguello PA, Gogos JA (2006) Modeling madness in mice: One piece at a time. *Neuron* 52:179–196.
37. van den Buuse M (2010) Modeling the positive symptoms of schizophrenia in genetically modified mice: Pharmacology and methodology aspects. *Schizophr Bull* 36: 246–270.
38. Ennaceur A (2014) Tests of unconditioned anxiety—pitfalls and disappointments. *Physiol Behav* 135:55–71.
39. Weiss SM, Lightowler S, Stanhope KJ, Kennett GA, Dourish CT (2000) Measurement of anxiety in transgenic mice. *Rev Neurosci* 11:59–74.
40. Maren S, Phan KL, Liberzon I (2013) The contextual brain: Implications for fear conditioning, extinction and psychopathology. *Nat Rev Neurosci* 14:417–428.
41. Herry C, Johansen JP (2014) Encoding of fear learning and memory in distributed neuronal circuits. *Nat Neurosci* 17:1644–1654.
42. Thompson RF, Spencer WA (1966) Habituation: A model phenomenon for the study of neuronal substrates of behavior. *Psychol Rev* 73:16–43.
43. Platel A, Porsolt RD (1982) Habituation of exploratory activity in mice: A screening test for memory enhancing drugs. *Psychopharmacology (Berl)* 78:346–352.
44. Leussis MP, Bolivar VJ (2006) Habituation in rodents: A review of behavior, neurobiology, and genetics. *Neurosci Biobehav Rev* 30:1045–1064.
45. Terzian AL, Drago F, Wotjak CT, Micale V (2011) The dopamine and cannabinoid interaction in the modulation of emotions and cognition: Assessing the role of cannabinoid CB1 receptor in neurons expressing dopamine D1 receptors. *Front Behav Neurosci* 5:49–59.
46. Tang YP, et al. (1999) Genetic enhancement of learning and memory in mice. *Nature* 401:63–69.
47. Milligan SR, Sales GD, Khirnykh K (1993) Sound levels in rooms housing laboratory animals: An uncontrolled daily variable. *Physiol Behav* 53:1067–1076.
48. Crabbe JC, Wahlsten D, Dudek BC (1999) Genetics of mouse behavior: Interactions with laboratory environment. *Science* 284:1670–1672.
49. Wahlsten D, et al. (2003) Different data from different labs: Lessons from studies of gene-environment interaction. *J Neurobiol* 54:283–311.
50. Goto Y, Yang CR, Otani S (2010) Functional and dysfunctional synaptic plasticity in prefrontal cortex: Roles in psychiatric disorders. *Biol Psychiatry* 67:199–207.
51. Crabtree GW, Gogos JA (2014) Synaptic plasticity, neural circuits, and the emerging role of altered short-term information processing in schizophrenia. *Front Synaptic Neurosci* 6:28–55.
52. Abbott LF, Varela JA, Sen K, Nelson SB (1997) Synaptic depression and cortical gain control. *Science* 275:220–224.
53. Herry C, Garcia R (2002) Prefrontal cortex long-term potentiation, but not long-term depression, is associated with the maintenance of extinction of learned fear in mice. *J Neurosci* 22:577–583.
54. Hansel D, Mato G (2013) Short-term plasticity explains irregular persistent activity in working memory tasks. *J Neurosci* 33:133–149.
55. Lewis DA, Gonzalez-Burgos G (2008) Neuroplasticity of neocortical circuits in schizophrenia. *Neuropsychopharmacol* 33:141–165.
56. Bicks LK, Koike H, Akbarian S, Morishita H (2015) Prefrontal cortex and social cognition in mouse and man. *Front Psychol* 6:1805–1820.
57. Drew LJ, et al. (2011) Evidence for altered hippocampal function in a mouse model of the human 22q11.2 microdeletion. *Mol Cell Neurosci* 47:293–305.
58. Schulz PE, Fitzgibbons JC (1997) Differing mechanisms of expression for short- and long-term potentiation. *J Neurophysiol* 78:321–334.
59. Volianskis A, Jensen MS (2003) Transient and sustained types of long-term potentiation in the CA1 area of the rat hippocampus. *J Physiol* 550:459–492.
60. Christianson JC, et al. (2011) Defining human ERAD networks through an integrative mapping strategy. *Nat Cell Biol* 14:93–105.
61. Horton AC, et al. (2005) Polarized secretory trafficking directs cargo for asymmetric dendrite growth and morphogenesis. *Neuron* 48:757–771.
62. Wayman GA, et al. (2006) Activity-dependent dendritic arborization mediated by CaM-kinase I activation and enhanced CREB-dependent transcription of Wnt-2. *Neuron* 50:897–909.
63. Junes-Gill KS, et al. (2011) hHSS1: A novel secreted factor and suppressor of glioma growth located at chromosome 19q13.33. *J Neurooncol* 102:197–211.
64. Dziembowska M, et al. (2012) Activity-dependent local translation of matrix metalloproteinase-9. *J Neurosci* 32:14538–14547.
65. Lu Y, Christian K, Lu B (2008) BDNF: A key regulator for protein synthesis-dependent LTP and long-term memory? *Neurobiol Learn Mem* 89:312–323.
66. Sanders SJ, et al.; Autism Sequencing Consortium (2015) Insights into autism spectrum disorder genomic architecture and biology from 71 risk loci. *Neuron* 87:1215–1233.
67. Mukai J, et al. (2015) Molecular substrates of altered axonal growth and brain connectivity in a mouse model of schizophrenia. *Neuron* 86:680–695.
68. Mukai J, et al. (2008) Palmitoylation-dependent neurodevelopmental deficits in a mouse model of 22q11 microdeletion. *Nat Neurosci* 11:1302–1310.
69. Tamura M, Mukai J, Gordon JA, Gogos JA (2016) Developmental inhibition of Gsk3 rescues behavioral and neurophysiological deficits in a mouse model of schizophrenia predisposition. *Neuron* 89:1100–1109.
70. Lek M, et al.; Exome Aggregation Consortium (2016) Analysis of protein-coding genetic variation in 60,706 humans. *Nature* 536:285–291.
71. CNV and Schizophrenia Working Groups of the Psychiatric Genomics Consortium; Psychosis Endophenotypes International Consortium (2017) Contribution of copy number variants to schizophrenia from a genome-wide study of 41,321 subjects. *Nat Genet* 49:27–35.
72. Rees E, et al.; Wellcome Trust Case Control Consortium (2014) Evidence that duplications of 22q11.2 protect against schizophrenia. *Mol Psychiatry* 19:37–40.
73. de Jong JW, et al. (2015) Reducing ventral tegmental dopamine D2 receptor expression selectively boosts Incentive Motivation. *Neuropsychopharmacol* 40:2085–2095.
74. Ferrés-Coy A, et al. (2016) Therapeutic antidepressant potential of a conjugated siRNA silencing the serotonin transporter after intranasal administration. *Mol Psychiatry* 21:328–338.
75. Sztainberg Y, et al. (2015) Reversal of phenotypes in MECP2 duplication mice using genetic rescue or antisense oligonucleotides. *Nature* 528:123–126.
76. Armbrecht HJ, et al. (2015) Antisense against amyloid-β protein precursor reverses memory deficits and alters gene expression in neurotropic and insulin-signaling pathways in SAMP8 mice. *J Alzheimers Dis* 46:535–548.
77. Miller TM, et al. (2013) An antisense oligonucleotide against SOD1 delivered intrathecally for patients with SOD1 familial amyotrophic lateral sclerosis: A phase 1, randomised, first-in-man study. *Lancet Neurol* 12:435–442.
78. Harshyne LA, et al. (2015) Glioblastoma exosomes and IGF-1R/AS-ODN are immunogenic stimuli in a translational research immunotherapy paradigm. *Cancer Immunol Immunother* 64:299–309.
79. Nelson CE, et al. (2016) In vivo genome editing improves muscle function in a mouse model of Duchenne muscular dystrophy. *Science* 351:403–407.
80. Tabebordbar M, et al. (2016) In vivo gene editing in dystrophic mouse muscle and muscle stem cells. *Science* 351:407–411.
81. Kondo A, et al. (2015) Antibody against early driver of neurodegeneration cis P-tau blocks brain injury and tauopathy. *Nature* 523:431–436.
82. Hawkes N (2015) Hopes rise for new Alzheimer's drug after secondary analysis. *BMJ* 351:4048–4049.